

Kullback-Leibler cluster entropy to quantify volatility correlation and risk diversity

L. Ponta
Università di Genova, Italy

A. Carbone
Politecnico di Torino, Italy

The *Kullback-Leibler cluster entropy* $\mathcal{D}_C[P||Q]$ is evaluated for the empirical and model probability distributions P and Q of the clusters formed in the *realized volatility* time series of five assets (SP&500, NASDAQ, DJIA, DAX, FTSEMIB). The Kullback-Leibler functional $\mathcal{D}_C[P||Q]$ provides complementary perspectives about the stochastic volatility process compared to the Shannon functional $\mathcal{S}_C[P]$. While $\mathcal{D}_C[P||Q]$ is maximum at the short time scales, $\mathcal{S}_C[P]$ is maximum at the large time scales leading to complementary optimization criteria tracing back respectively to the maximum and minimum relative entropy evolution principles. The realized volatility is modelled as a time-dependent fractional stochastic process characterized by power-law decaying distributions with positive correlation ($H > 1/2$). As a case study, a multiperiod portfolio built on diversity indexes derived from the Kullback-Leibler entropy measure of the *realized volatility*. The portfolio is robust and exhibits better performances over the horizon periods. A comparison with the portfolio built either according to the uniform distribution or in the framework of the Markowitz theory is also reported.

I. INTRODUCTION

Information theoretic concepts based on the Kullback-Leibler functionals are increasingly finding applications in several contexts [1–5]. Insightful perspectives on the dynamics underlying stochastic processes can be taken in terms of entropy evolution [6]. According to the second law of thermodynamics, the Shannon-Gibbs entropy S increases over time and reaches a *maximum value* S_{max} corresponding to a steady-state. Entropy functionals are expressed in terms of probability distribution functions P of the thermodynamic state. However, probability distributions are barely defined when empirical real world data are concerned. In such circumstances, the procedure of *coarse-graining* is implemented by partitioning the phase space into discrete not overlapping cells C_j . Measures μ can be defined over the cell j satisfying the condition $0 < \mu(C_j) < \mu(X)$ for all j . The *coarse-grained distribution* $P(\mu(C_j))$ is entered in the entropy functional yielding a so called *coarse-grained entropy* \mathcal{S} equal or larger than S the entropy analytically defined for the same system.

Time series of random variables x_t provide relevant observables of the system dynamics at subsequent time instances t . Coarse-graining is obtained by cutting sequential segments $x_{t'} = x_t x_{t+1} \dots x_{t'-1}, t < t'$ of varying lengths out of the time series x_t [8, 9]. Then the entropy evolution for the coarse grained sequence x_t is estimated at varying *block size*. Such coarse-grained information measure is commonly referred to as *block entropy*. Coarse-graining via *density-based clustering* consists in intersecting empirical and thresholding data sets. The intersections define the clusters (cells) which are not affected by the drawbacks of the standard *center-based* clusters. Sample by sample estimates of the probability distribution of *density-based cluster features* are increasingly proved useful when large amount of data should be

investigated. Entropy measures implemented on density-based cluster probabilities have emerged as a promising area of complexity science and statistical machine learning (*Information theoretic clustering*) [10–14].

The *cluster entropy* approach adopted in this work operates via a density-based partition obtained by intersecting empirical data (e.g. a time series) with a pointwise threshold defined by a time dependent average [15, 16]. The extent to which the cluster entropy exceeds the value expected by the analytic Shannon functional has been discussed in [17] where the approach has been implemented on human chromosome sequences. The *Kullback-Leibler cluster entropy* [18] estimates the divergence between the probability distributions P and Q respectively of the empirical and artificial cluster sequences taken as a model. How the *Kullback-Leibler cluster entropy* can be used to infer the optimal distribution P has been demonstrated for fractional Brownian processes (fBm) with H the Hurst exponent in the range $H \in [0, 1]$ [18]. Keeping in mind the general property of the relative entropy to reach its maximum value at short time scales and evolve towards the minimum (zero) for $P = Q$ [2, 7], the Kullback-Leibler cluster entropy complements the Shannon cluster entropy, a proxy of correlation at large time scales.

In economics and finance, entropy tools are adopted for asset pricing models, risk assessment and wealth allocation motivated by the concept that entropy itself is a measure of diversity [19–23]. Contrarily to the time series of prices widely recognised to behave as simple Brownian motions with Hurst exponent $H \sim 1/2$, the mechanisms of long-term correlation underlying the stochastic dynamics of the volatility (i.e. the time series corresponding roughly to the local variance of the price time series) are still debated. Volatility has been modelled as a positively correlated fractional Brownian motions with $H > 1/2$ [24]. An anticorrelated stochastic process with

$H < 1/2$ has been proposed with the market prices being a semimartingale with $H \sim 1/2$ [25]. Numerical experiments reported in [26] show that the volatility exhibits Hurst exponent $H < 1/2$ though its microscopic origin might be an artifact. This work intends to contribute to the debate by exploiting the inferential ability of the Kullback-Leibler cluster entropy. To this scope the probability distributions estimated respectively in the *realized volatility* series of five financial assets and in fully uncorrelated Brownian motions are compared to each other.

Diversity measures derived from various entropy functionals have been proposed to quantify compositional heterogeneity of natural and man-made complex systems [27–29]. The measures adopt the *maximum entropy* as a proxy of *maximum diversity* consistently with the spreading of the distribution compared to the uniform or delta ones [28]. The concept of diversity has been originally adopted in finance in the portfolio theory framework pioneered by Markowitz [30–32]. First attempts of using information theoretic tools for risk assessment and wealth allocation consisted in the introduction of the Markowitz mean-variance weights w_i into the Shannon entropy functional:

$$S(w_i) = - \sum_{i=1}^{\mathcal{A}} w_i \log w_i \quad , \quad (1)$$

where \mathcal{A} is the number of assets. Eq. (1) ranges between the maximum value $S(w_i) = \log \mathcal{A}$ when $w_i = 1/\mathcal{A}$ (*equally weighted assets*) and the minimum $S(w_i) = 0$ when $w_i = 1$ for one asset and $w_i = 0$ for all the others. The Kullback-Leibler entropy functional has been used to quantify the divergence of the Markowitz weights w_i with respect to the uniformly distributed weights $u_i = 1/\mathcal{A}$:

$$D(w_i, u_i) = \sum_{i=1}^{\mathcal{A}} w_i \log \frac{w_i}{u_i} \quad . \quad (2)$$

Though the entropy functionals could mitigate strong fluctuations and biases towards riskiest markets, the relationships (1,2) still embed the weights w_i estimated under the wrong belief of stationary normally distributed return. Diversity measures suitable to capture the complexity of composite micro- and macro-economic features still remains an open challenge [29]. The Kullback-Leibler cluster entropy will be used to define a robust and sound set of diversity measures built upon the coarse grained probability distribution of the realized volatility of tick-by-tick data of the Standard & Poor 500 (SP&500), Dow Jones Ind. Avg (DJIA), Deutscher Aktienindex (DAX), Nasdaq Composite (NASDAQ), Milano Indice di Borsa (FTSEMIB) assets.

The manuscript is organized as follows. Section II A includes the main notions and computational steps underlying the Kullback-Leibler cluster divergence approach. Section II B describes the construction of the diversity measures in terms of the relative cluster entropy. Section III illustrates the approach on volatility series of tick-by-tick data of the Standard & Poor 500 (SP&500), Dow

Jones Ind. Avg (DJIA), Deutscher Aktienindex (DAX), Nasdaq Composite (NASDAQ), Milano Indice di Borsa (FTSEMIB) assets. The Kullback-Leibler cluster entropy and the diversity indexes are estimated over twelve monthly periods covering the year 2018. A comparison with the measures obtained by using the Shannon cluster entropy, the equally-weighted and the Sharpe ratio estimates are also included. In Section IV the implications of the study are shortly discussed. A numerical example of investment is also provided. Conclusions are drawn in Section V.

II. METHODS

A few definitions and the main computational steps of the *Kullback-Leibler cluster entropy* approach are summarized in subsection II A. The construction of the *Kullback-Leibler diversity index* is reported in subsection II B.

A. Kullback-Leibler Cluster Entropy

As mentioned in the introduction, the evaluation of the entropy functional for real-world problems requires the procedure of partitioning the data set (coarse-graining) to yield the coarse-grained probability distribution of cells C_j .

In this work, the focus is on empirical time series of the realized volatility where the partition is obtained by intersecting the data with a pointwise threshold *density-based clustering*. Consider a time series $\{x_t\}$ of length N . The local average

$$\tilde{x}_{t,n} = \frac{1}{n} \sum_{n'=0}^{n-1} x(t-n') \quad (3)$$

generates a family of time series of length $N - n$ for $n \in (1, N)$. It is $\tilde{x}_{t,n} = \{x_t\}$ for $n = 1$ and $\tilde{x}_{t,n} = \text{constant}$ for $n = N$. Consequently, a family of partition $\{\mathcal{C}\} = \{\mathcal{C}_{n,1}, \mathcal{C}_{n,2}, \dots, \mathcal{C}_{n,j}, \dots\}$ of non-overlapping clusters is generated by the intersections of $\{x_t\}$ and $\{\tilde{x}_{t,n}\}$. Each cluster $\mathcal{C}_{n,j}$ is defined by the condition $\epsilon_{t,n} = x_t - \tilde{x}_{t,n} = 0$ for each n . The clusters are characterized by the *duration* $\tau_j \equiv \|t_j - t_{j-1}\|$, with the instances t_{j-1} and t_j corresponding to subsequent intersection pairs. The coarse grained distribution of the cluster durations $P(\tau_j, n)$ is obtained by ranking the number of clusters $\mathcal{N}(\tau_j, n)$ according to their duration τ_j :

$$P(\tau_j, n) = \frac{\mathcal{N}(\tau_j, n)}{\mathcal{N}_C(n)} \quad (4)$$

with $\mathcal{N}_C(n) = \sum_j \mathcal{N}(\tau_j, n)$ the number of clusters generated for each value of the parameter n . The total number of clusters for all the possible values of the parameter n

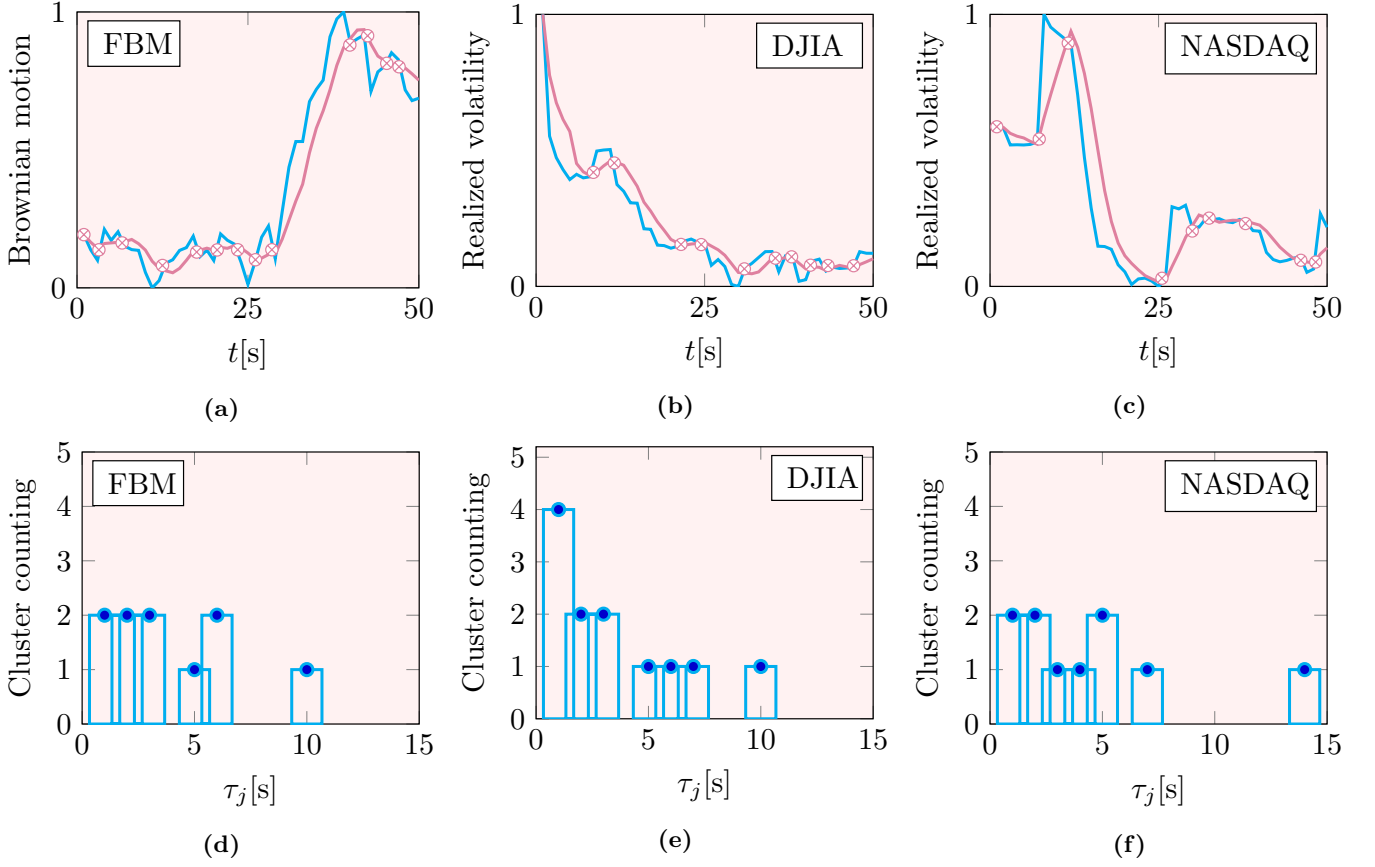


FIG. 1: **Concept sketch of the Kullback-Leibler cluster method.** Top Panels: samples of the (a) model time series - an artificially generated Brownian motion with $H = 0.5$ (FBM), of the realized volatility series of (b) DJIA and (c) NASDAQ assets (blue lines). Sample lengths is $N = 50$. The moving average with $n = 5$ is plotted for each time series (purple lines). The clusters, formed at the intersections of each series and moving average, are indicated by crossed circles. Bottom Panels: The clusters formed in (a),(b) and (c) are counted according to their length. The cluster occurrences are plotted in the bottom panels respectively for the FBM (d), DJIA (e) and NASDAQ (f). The cluster counts represent the archetypes of the probability distribution P and Q to be introduced in the Kullback-Leibler expression (Eq. (6)).

is defined as: $\mathcal{N}_C = \sum_{n=1}^N \mathcal{N}_C(n)$. The normalization condition holds as usual:

$$\sum_{n=1}^N \sum_{j=1}^{\mathcal{N}_C(n)} P(\tau_j, n) = 1. \quad (5)$$

Next consider a coarse grained distribution function $Q(\tau_j, n)$ generated by a model of the time series $\{x_t\}$. The *relative cluster entropy* or *cluster divergence* can be defined in terms of the Kullback-Leibler functional of the probabilities $P(\tau_j, n)$ and $Q(\tau_j, n)$:

$$\mathcal{D}_{j,n}[P||Q] = P(\tau_j, n) \log \frac{P(\tau_j, n)}{Q(\tau_j, n)}, \quad (6)$$

with the condition $\text{supp}(P) \subseteq \text{supp}(Q)$. By summing (6) over all the cluster durations τ_j and all the partitions

generated by varying the parameter n , one has:

$$\mathcal{D}_C[P||Q] = \sum_{n=1}^N \sum_{j=1}^{\mathcal{N}_C(n)} P(\tau_j, n) \log \frac{P(\tau_j, n)}{Q(\tau_j, n)}. \quad (7)$$

which quantifies the information yield when the empirical probability distribution P is compared to the model probability distribution Q [18].

For illustrative purposes, short samples (50 points) of time series are plotted in Figs. 1(a),(b),(c). The time series taken as a model is a Fractional Brownian motion (FBM) with Hurst exponent $H = 0.5$ (blue line in Fig. 1 (a)). The empirical time series to be analysed are the realized volatility of DJIA (blue line in Fig. 1 (b)) and NASDAQ (blue line in Fig. 1 (c)). The intersection (crossed circles) with the moving average curves (purple lines) generate clusters of different lengths. The clusters are counted according to their lengths to build the prototypical probability distributions to be entered in the

Eqs. (6,7) and are respectively shown in Figs. 1(d),(e),(f).

To further illustrate how the relative cluster entropy operates, Eq. (7) is written in terms of continuous variables:

$$D_C[P||Q] = \int P(\tau) \log \frac{P(\tau)}{Q(\tau)} d\tau . \quad (8)$$

For power-law probability distributions:

$$P(\tau) = \frac{\alpha_1 - 1}{\tau_{\min}} \left(\frac{\tau}{\tau_{\min}} \right)^{-\alpha_1} \quad Q(\tau) = \frac{\alpha_2 - 1}{\tau_{\min}} \left(\frac{\tau}{\tau_{\min}} \right)^{-\alpha_2} \quad (9)$$

where $\alpha_1 > 1$ and $\alpha_2 > 1$ are the correlation exponents and $\tau \in [1, \infty]$. After integration between $\tau_{\min} = 1$ and $\tau_{\max} = \infty$, Eq. (8) writes:

$$D_C[P||Q] = \log \frac{\alpha_1 - 1}{\alpha_2 - 1} - \frac{\alpha_1 - \alpha_2}{\alpha_1 - 1} \quad (10)$$

where the condition $D_C(\infty) = 0$ has been used to evaluate the integration constant. The cluster formation process (coarse-graining) based on the intersection of a time series x_t and the moving average $\tilde{x}_{t,n}$ described at the beginning of this section can be further understood in the general context of *first passage problems* [33] with particular reference to the case of fractional Brownian motions [34]. The probability distribution functions of the cluster duration τ is a power-law with exponent $\alpha = 2 - H$ where $H \in [0, 1]$ is the Hurst exponent of the fractional Brownian motion generating the clusters [15]. Thus by using $\alpha_1 = 2 - H_1$ and $\alpha_2 = 2 - H_2$, Eq. (10) writes:

$$D_C[P||Q] = \log \frac{1 - H_1}{1 - H_2} + \frac{H_1 - H_2}{1 - H_1} . \quad (11)$$

Eq. (10) turns out to depend only on the exponents α_1 and α_2 of the power law distributions of the empirical and model sequences. Eq. (11) turns out to depend only on H_1 and H_2 , respectively the Hurst exponent of the empirical and model sequences.

$D_C[P||Q]$ satisfies the general property of the relative entropy to be positive defined:

$$D_C[P||Q] \geq 0 \quad (12)$$

over the whole range of $\alpha_1 = 2 - H_1$ and $\alpha_2 = 2 - H_2$. The minimum value:

$$D_C[P||Q] = 0 \quad (13)$$

is obtained for $H_1 = H_2$ ($\alpha_1 = \alpha_2$).

Eqs. (10,11) could be interpreted as an inferential measure of the correlation exponent α and of the Hurst exponent H for fractional Brownian motions. The functionals $\mathcal{D}_{j,n}[P||Q]$ defined in Eq. (6) are the individual components of the relative cluster entropy. $\mathcal{D}_{j,n}[P||Q]$ are dependent on the Hurst exponent and can be separated into positive or negative contributions respectively for positive and negative correlated sequences. It is worth remarking that the functionals $\mathcal{D}_{j,n}[P||Q]$ depend on the cluster time scale τ_j .

B. Kullback-Leibler cluster diversity index

The *relative cluster entropy index* $I_{\mathcal{D}}$ can be defined in terms of the Eqs. (6,7) as:

$$I_{\mathcal{D}} = \sum_{n=1}^N \sum_{j=1}^m D(\tau_j, n) + \sum_{n=1}^N \sum_{j=m}^N D(\tau_j, n) . \quad (14)$$

The first term on the right hand side of Eq. (14) refers to the sum of $D(\tau_j, n)$ over cluster lifetimes in the range $1 < \tau_j < \tau_m < n$ where $D(\tau_j, n) \neq 0$ varies from the maximum for $\tau_j \rightarrow 1$ to the minimum value $D(\tau_j, n) \rightarrow 0$ for $\tau_j = \tau_m \approx n$. The second term corresponds to cluster lifetimes in the range $n < \tau_j < N$ where $D(\tau_j, n) \approx 0$.

$I_{\mathcal{D}}$ is a measure of diversity, suitable to compare cluster probabilities generated in different sequences. To this purpose, the index $I_{\mathcal{D}}$ must be normalized over the ensemble to be compared. The normalized indexes (*Kullback-Leibler weights*) are defined as follows:

$$w_{i,\mathcal{D}} = \frac{I_{i,\mathcal{D}}^{-1}}{\sum_{i=1}^A I_{i,\mathcal{D}}^{-1}} , \quad (15)$$

that satisfy the conditions $\sum_{i=1}^A w_{i,\mathcal{D}} = 1$ and $w_{i,\mathcal{D}} \geq 0$. The weights $w_{i,\mathcal{D}}$ allow to compare and rank time series with reference to an artificial time series taken as a model.

In section III, the relative cluster entropy approach will be used to quantify the divergence of the correlation exponents of the realized volatility series of five assets. Eqs. (6,7) will be used to quantify the correlation exponent H_1 of the empirical sequence in comparison to a fractional Brownian motion with assigned Hurst exponent H_2 taken as a model. We will also estimate the *relative cluster entropy index* $I_{\mathcal{D}}$ and build a numerical example of a portfolio with the cluster weights $w_{i,\mathcal{D}}$ given in Eq. (15) to five financial assets.

III. RESULTS

The *relative cluster entropy* approach will be implemented to analyse the correlation degree of the realized volatility series of five assets. For the sake of clarity, the definitions of return and realized volatility are shortly recalled. Given a time series of market price p_t , the *return time series* is defined as:

$$r_t = \log p_t - \log p_{t-1} . \quad (16)$$

The *realized volatility time series* is defined as:

$$\sigma_{t,T} = \sqrt{\frac{\sum_{t=k}^{k+T} (r_t - \mu_{t,T})^2}{T-1}} , \quad (17)$$

where T is the volatility window and $\mu_{t,T}$ is the time series of the *expected return* over T :

$$\mu_{t,T} = \frac{1}{T} \sum_{t=k}^{k+T} r_t . \quad (18)$$

	(a)	(b)	(c)	p_1	p_2	p_3	p_4	p_5	p_6	p_7	p_8	p_9	p_{10}	p_{11}	p_{12}
NASDAQ	2570	6982017	USD	7007	7386	7181	6870	7131	7554	7568	7707	8091	8037	7434	7442
S&P500	505	6142443	USD	2696	2822	2678	2582	2655	2735	2727	2813	2897	2925	2740	2790
DJIA	30	5749145	USD	24824	26187	24609	23644	24099	24635	24307	25334	25952	26651	25381	25826
DAX	30	7859601	USD	26	28	25	25	25	25	24	25	24	24	22	22
FTSEMIB	40	11088322	USD	28268	27576	27684	27697	28462	24920	25689	24668	23750	22349	21941	21460

TABLE I: **Asset Data.** Member firms constituting the asset (a). Number of price ticks for the year 2018 (b). Currency (c). Adjusted close price on the first available day for each month of the year 2018 ($p_1 \dots p_{12}$).

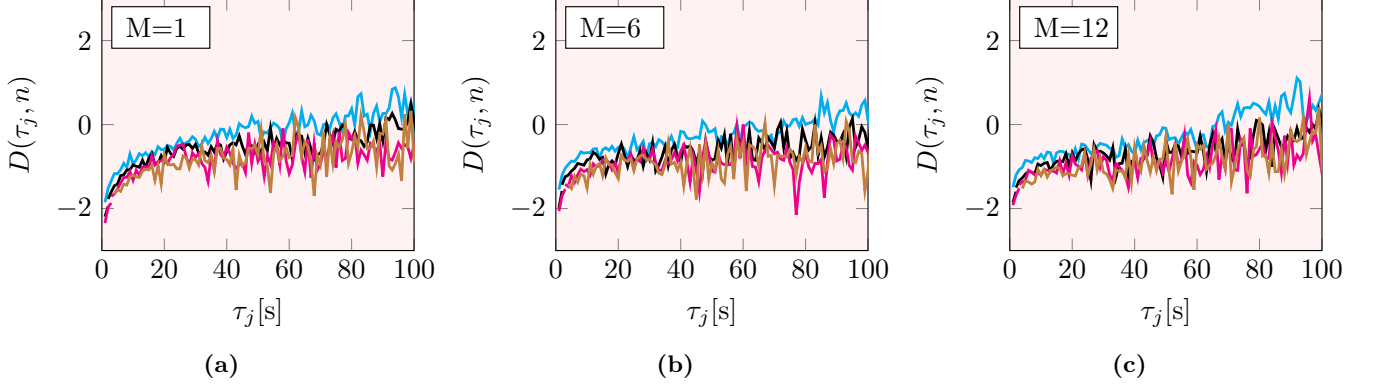


FIG. 2: **Kullback-Leibler cluster entropy functional $\mathcal{D}(\tau_j, n)$ vs cluster duration.** Each curve is estimated by means of Eq. (6) the Kullback-Leibler functional of $P(\tau_j, n)$ the empirical probability distribution of the size of the clusters of the volatility series of the market S&P500. $Q(\tau_j, n)$ is the probability distribution of the cluster size of a synthetic fractional Brownian motion with $H = 0.5$. Time series have length $N = 492023$. Volatility is estimated according to Eq. (17) with window $T = 180s$ for the three graphs. Plots refer respectively to one ($\mathcal{M} = 1$)(a), six ($\mathcal{M} = 6$) (b) and twelve ($\mathcal{M} = 12$) (c) monthly periods sampled out of the year 2018. Different curves in the same plot refer to different values of the moving average window n ranging from 50s to 200s with step 50s.

Eq. (17) corresponds to the estimate of the variance of return over the volatility window T [35, 36].

The analysis are carried on tick-by-tick data of the S&P500, NASDAQ, DJIA, DAX and FTSEMIB assets (details in Table I). Short samples of length $N = 50$ of the realized volatility time series of the DJIA and NASDAQ assets are plotted in Figs. 1(b),(c). The model series is a fractional Brownian motion FBM with $H = 0.5$. A short sample of length $N = 50$ of the FBM is plotted in Fig. 1(a). Blue lines represent the time series x_t , purple line represents the moving average $\tilde{x}_{t,n}$ with $n = 5$. The clusters are formed by the intersections of the series and its moving average. The crossing points are drafted as *otimes* symbols in Figs. 1 (a),(b),(c). The clusters are counted and ranked according to their length. The frequencies of cluster occurrence of Fig. 1 (a),(b),(c) are plotted as a function of the cluster duration τ_j respectively in Figs. 1(d),(e),(f). These plots are intended as simplistic illustrations of the probability distribution functions $Q(\tau_j, n)$ and $P(\tau_j, n)$ appearing in the Eqs. (6,7).

The functionals $\mathcal{D}(\tau_j, n)$ defined by Eqs. (6) are estimated for the *realized volatility* series of the financial market data described in Table I. Results for the S&P500 market are plotted in Fig. 2 (a), (b) and (c). The volatility window is $T = 180s$. The volatility is estimated

over different monthly horizons \mathcal{M} . Time horizons are $\mathcal{M} = 1$, $\mathcal{M} = 6$ and $\mathcal{M} = 12$ months respectively for Figs. 2 (a)(b)(c). Analogous results have been obtained for the *realized volatility* of the NASDAQ, DJIA, DAX and FTSEMIB assets. The behaviour of the $\mathcal{D}(\tau_j, n)$ curves in Fig. 2 (a)(b)(c) is consistent with the properties expected for relative entropy functionals. In particular, $\mathcal{D}(\tau_j, n)$ is maximum at small τ_j , then decreases towards the minimum values at large cluster durations $\mathcal{D}(\tau_j, n) \rightarrow 0$ as τ_j increases. The maximum values of $\mathcal{D}(\tau_j, n)$ at small τ_j is consistent with the loss of power-law correlation and the onset of exponential correlation at cluster duration τ_j larger than n . The divergence components $\mathcal{D}(\tau_j, n)$ plotted in Fig. 2 take negative values at the small τ_j pointing to a Hurst exponent H_1 larger than H_2 .

As a further remark, we note that the functionals $\mathcal{D}(\tau_j, n)$ are estimated on the *realized volatility* series of the financial market data, made stationary by the detrending procedure. The cluster relative entropy described in Section IIA is conditioned by the model probability Q , which is assumed to be a power law rather than on an unrealistic hypothesis of Gaussianity of returns.

Next, the weights $w_{i,\mathcal{D}}$ as defined by Eq. (15) are estimated for the realized volatility of the five assets. Results are plotted in Figs. 3(a),(b),(c). The weights

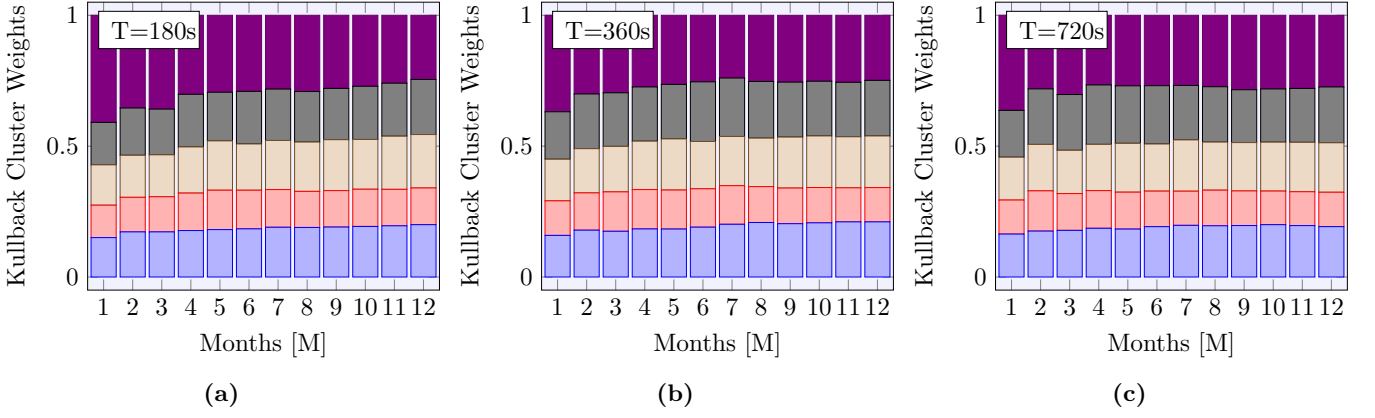


FIG. 3: **Kullback-Leibler weights $w_{i,\mathcal{D}}$ vs. investment horizon \mathcal{M} (monthly periods).** The weights have been estimated by using Eqs. (14,15) on the realized volatility respectively for the tick-by-tick series of the markets: S&P500 (■), NASDAQ (■), DJIA (■), DAX (■) and FTSEMIB (■). The time series of the realized volatility are estimated according to Eq. (17) respectively with window $T = 180s$ (a), $T = 360s$ (b) and $T = 720s$ (c).

are estimated for temporal horizons \mathcal{M} ranging between one and twelve months. Plots correspond to three values of the volatility window $T = 180s$ (a), $T = 360s$ (b) and $T = 720s$ (c). At short investment horizons \mathcal{M} and small volatility windows T , the weights deviate from the u_i values corresponding to uniformly allocated wealth. As \mathcal{M} and T increase, the weights tend towards the uniform distribution consistently with the increased level of surprise with the spreading of cluster duration τ_j . A distribution of weights close to u_i , is related to the reduced predictability at longer horizons and larger volatility windows. This feature can be quantitatively interpreted bearing in mind that the empirical probability distribution and the model distribution become closer to each other at large cluster durations.

To further clarifying the meaning of the results reported in Fig. 2 and Fig. 3, the *Shannon cluster entropy* approach has been implemented on the realized volatility of the five markets. The *Shannon cluster entropy* $\mathcal{S}_C[P]$ is obtained by introducing the cluster probability distribution of the *realized volatility* $P(\tau_j, n)$ in the Shannon functional:

$$\mathcal{S}_{j,n}[P] = -P(\tau_j, n) \log P(\tau_j, n) . \quad (19)$$

Upon summing $\mathcal{S}_{j,n}[P]$ over all the instances of cluster duration τ_j for all the partitions generated by varying the parameter n , the *cluster entropy* writes:

$$\mathcal{S}_C[P] = - \sum_{n=1}^N \sum_{j=1}^{N_C(n)} P(\tau_j, n) \log P(\tau_j, n) . \quad (20)$$

A *cluster entropy index* I_S has been defined by integrating the Shannon cluster entropy functional [37, 38]:

$$I_S = \sum_{n=1}^N \sum_{j=1}^m \mathcal{S}(\tau_j, n) + \sum_{n=1}^N \sum_{j=m}^N \mathcal{S}(\tau_j, n) , \quad (21)$$

Eq. (21) has been written in Refs. [37, 38] with the sums over the moving average n and lifetime τ_j implemented in two steps. To improve readability of Eq. (21), the sums are gathered together, the index i is dropped, and the suffix \mathcal{S} is added to distinguish I_S from the index $I_{\mathcal{D}}$ derived in the previous section. The index defined in Eq. (21) must be normalized over the ensemble:

$$w_{i,\mathcal{S}} = \frac{I_{i,\mathcal{S}}}{\sum_{i=1}^{\mathcal{A}} I_{i,\mathcal{S}}} , \quad (22)$$

The normalized index are called *Shannon cluster weights* and satisfy the conditions $\sum_{i=1}^{\mathcal{A}} w_{i,\mathcal{S}} = 1$ and $w_{i,\mathcal{S}} \geq 0$. By using Eq. (21), diversity can be quantified by maximizing the cluster entropy of *return* and *volatility* of the \mathcal{A} assets at different temporal horizons \mathcal{M} .

The results obtained by implementing Eq. (19) on the *realized volatility* of the S&P500 asset are shown in Fig. 4 respectively for the horizons $\mathcal{M} = 1$ (a), $\mathcal{M} = 6$ (b) and $\mathcal{M} = 12$ (c) months. The volatility window is $T = 180s$ for the three panels. Next, the weights $w_{i,\mathcal{S}}$ are estimated by using Eq. (22). The weights $w_{i,\mathcal{S}}$ are shown in Fig. 5 for $\mathcal{M} = 1$ to $\mathcal{M} = 12$ and volatility windows $T = 180s$ (a), $T = 360s$ (b), $T = 720s$ (c).

A comparison with the weights w_i yielded by the traditional mean-variance Markowitz approach [30] is also reported. The weights w_i are chosen to minimize the variance $\sigma^2(r)$ of the return r given the mean $\mu(r)$ by maximizing the *Sharpe ratio*:

$$R_S = \frac{\mu(r)}{\sqrt{\sigma^2(r)}} . \quad (23)$$

The weights have been maximized on tick-by-tick data of the high-frequency markets described in Table I by using the MATLAB Financial Toolboxes [39]. Raw market data are sampled to yield equally spaced series with equal lengths. The sampling intervals are indicated by

Δ . The Sharpe ratio weights are estimated over multiple horizons \mathcal{M} (twelve monthly periods over the year 2018). Results are shown in Fig. 6 respectively for sampling interval $\Delta = 10s$ (a), $\Delta = 100s$ (b) and $\Delta = 1000s$ (c). One can note the high variability of the weights of the same asset over consecutive periods and biased distribution towards riskiest assets. Compared to Sharpe ratio weights w_i , the relative cluster entropy weights $w_{i,\mathcal{D}}$ exhibit less variability, with values smoothly approaching the equally distributed weights u_i as increasing investment horizons \mathcal{M} and volatility windows T are considered.

It is worth remarking that the definition of the weights is not unique and might be modified to privilege other investment strategies depending upon financial product specifications.

The weights $w_{i,\mathcal{D}}$ are defined in Eq. (15) in terms of the reciprocal of the entropy index $I_{i,\mathcal{D}}^{-1}$ whereas the weights $w_{i,\mathcal{S}}$ are defined in Eq. (22) in terms of $I_{i,\mathcal{S}}$. This difference is related to the complementary behaviour of the Kullback-Leibler and Shannon cluster entropies, in particular for what concern the dependence on the cluster duration τ_j at small and large scales.

The investment timeline has been split into periods of equal duration Θ (one month). The portfolio is evaluated over multiple time horizons $\mathcal{M} = \xi\Theta$. The different sets of vectors $w_i(\mathcal{M})$ represent the multi period portfolio which calibrates the long horizon weights over the short ones. In the next section, we will consider an investment timeline of one year with Θ equal to one month, then $\xi \in [1, 12]$ yielding investment horizons \mathcal{M} lasting from one to twelve months. Investors can choose among different alternatives of $w_i(\mathcal{M})$ according to their period preferences and the specificity of the investment products.

IV. DISCUSSION

In Section III, the stochastic volatility process of five assets has been investigated by adopting the Kullback-Leibler functional $\mathcal{D}_{j,n}[P||Q]$ and entropy $\mathcal{D}_C[P||Q]$ defined by the Eqs. (6,7). The *divergence* is quantified between the cluster probability distributions P of the *realized volatility* time series and Q of a fully uncorrelated process (a simple Brownian motion with $H = 1/2$ taken as reference). Results are shown in Fig. 2 (a),(b),(c). For comparison purposes, the realized volatility time series of the five assets have been further analysed by using Eqs. (19,20), i.e. the information theoretic measures based on the Shannon functional $\mathcal{S}_{j,n}[P]$ and entropy $\mathcal{S}_C[P]$. Results for S&P500 are shown in Fig. 4.

By comparing the curves in Fig. 2 with those in Fig. 4, one can note that the functionals $\mathcal{D}_{j,n}[P||Q]$ and $\mathcal{S}_{j,n}[P]$ exhibit a different dependence on $\tau_j \in [1, \infty]$. More specifically $\mathcal{D}_{j,n}[P||Q]$ is a decreasing function of τ_j , while $\mathcal{S}_{j,n}[P]$ increases as τ_j increases. The maximum of $\mathcal{D}_{j,n}[P||Q]$ occurs at short cluster duration ($\tau_j \rightarrow 1$). Then, $\mathcal{D}_{j,n}[P||Q]$ decreases as P approaches the fully un-

correlated probability distribution at large cluster duration τ_j . $\mathcal{D}_{j,n}[P||Q]$ takes larger values as the probability distribution P is strongly correlated (power-law correlated) compared to the uncorrelated distribution Q taken as reference. Conversely, the Shannon entropy functional is minimum ($\mathcal{S}_{j,n}[P] \sim \ln 1 = 0$) corresponding to the minimum uncertainty (minimum surprise) on the outcome of the cluster duration τ_j . If P is a fully developed power-law distribution defined over a large number of cluster sizes, the entropy approaches the maximum value corresponding to maximum uncertainty (maximum surprise) on the outcome at large cluster sizes. The increase is related to the power-law distribution spreading over a broad range of cluster values being the entropy a measure of the uncertainty (surprise) of the cluster size outcomes. In summary, while the Shannon cluster entropy takes its minimum value at short cluster duration τ_j , the Kullback-Leibler divergence is maximum at short lifetime and becomes negligible as cluster duration τ_j increases. Hence, the two measures provide complementary information when implemented on the same datasets. The different dependence of $\mathcal{D}_{j,n}[P||Q]$ and $\mathcal{S}_{j,n}[P]$ on τ_j are reflected in the Kullback-Leibler $\mathcal{D}_C[P||Q]$ and Shannon $\mathcal{S}_C[P]$ entropy, obtained by summing the functionals over the entire ensemble of clusters.

To avoid the impression that the information theoretic measure based on the Eqs. (6,7) might have only a speculative interest aimed at scrutinizing the roughness of the *realized volatility* time series, a practical metric has been developed leading to definition of the relationships Eqs. (15,14) for quantifying market risk and related wealth allocation. The index $I_{\mathcal{D}}$ and the set of weights $w_{i,\mathcal{D}}$ are estimated for the high-frequency market data series (details in Table I) over multiple consecutive horizons \mathcal{M} . The results are shown in Fig. 3. A continuous set of values of the weights $w_{i,\mathcal{D}}$ with a smooth and sound dependence on the horizon \mathcal{M} can be observed. The regularity and smoothness of the entropy-based estimate of the weights can be related to the stationary detrended distribution rather than the unrealistic mean-variance hypothesis of Gaussianity and stationarity of the return of the financial series. The proposed approach uses a stationary set of variables (i.e. the detrended clusters and their durations τ_j of the return and volatility series) rather than non-stationary and not-normal variables as asset returns and volatility. The relevance of the stationarity condition when relative entropy measures are adopted has been discussed in [3]. The relative cluster entropy weights $w_{i,\mathcal{D}}$ vary continuously and take values close to the equally distributed weights u_i . At short investment horizons \mathcal{M} , the weights $w_{i,\mathcal{D}}$ deviate more from the equally distributed values than they do at long investment horizons.

This behavior is consistent with the structure of the relative cluster entropy functional $\mathcal{D}(\tau_j, n)$ which maximizes the deviation of the cluster distribution at short τ_j duration as opposed to the $\mathcal{S}(\tau_j, n)$ functional which yields the maximum deviation at large τ_j values. Con-

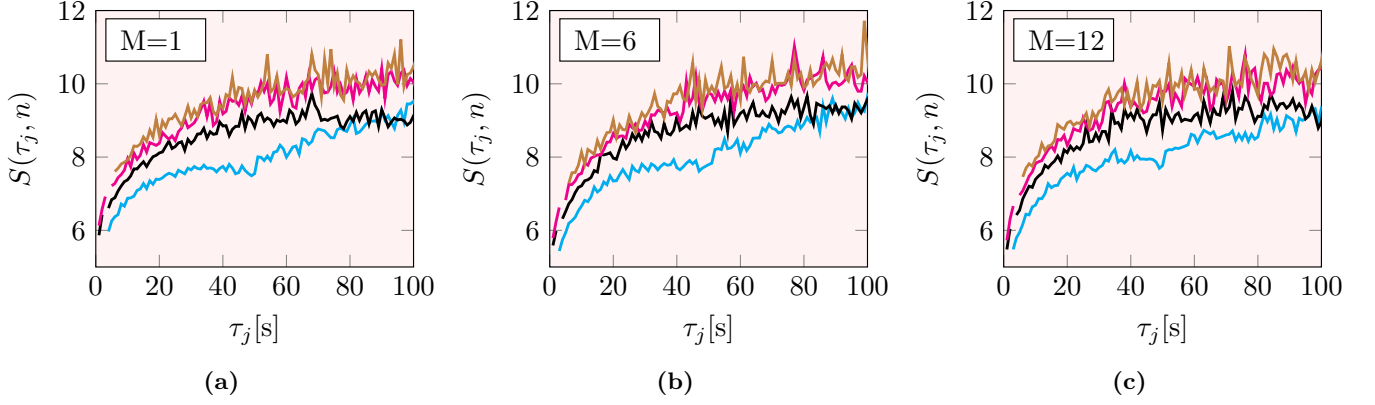


FIG. 4: **Shannon cluster entropy functional $\mathcal{S}(\tau_j, n)$ vs cluster duration.** Each curve is estimated by means of Eq. (19) based on the Shannon functional of $P(\tau_j, n)$ the probability distribution of the cluster duration of the volatility series of the S&P500 asset. Time series have length $N = 492023$. Volatility is estimated according to Eq. (17) with window $T = 180s$ for the three graphs. Plots refer respectively to one ($\mathcal{M} = 1$)(a), six ($\mathcal{M} = 6$)(b) and twelve ($\mathcal{M} = 12$)(c) monthly periods sampled out of the year 2018. Different curves in the same plot refer to different values of the moving average window n ranging from $50s$ to $200s$ with step $50s$.

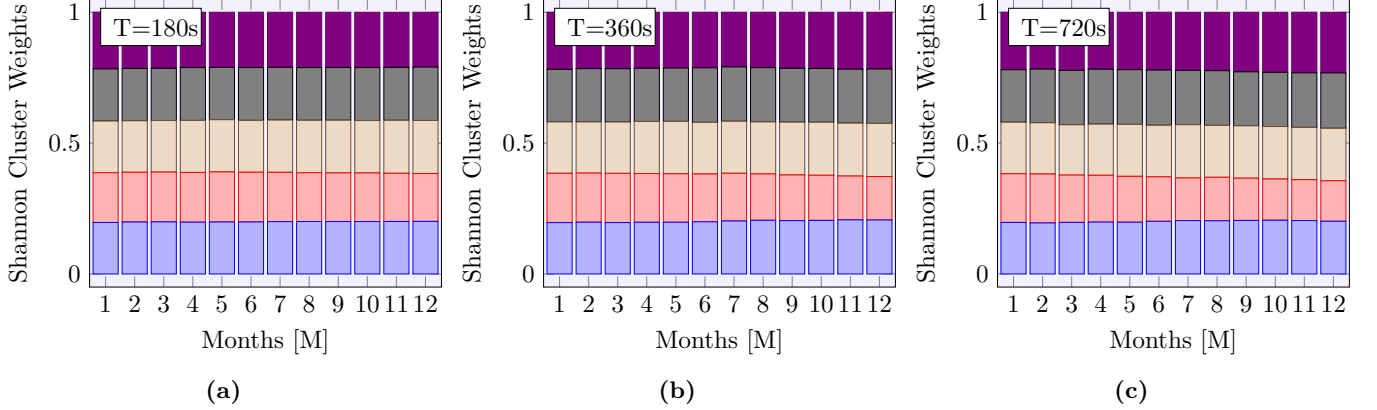


FIG. 5: **Shannon cluster weights $w_{i,S}$ vs. investment horizon \mathcal{M} (monthly periods).** The weights have been estimated by applying Eq. (22) to the realized volatility respectively for the tick-by-tick market series: S&P500 (■); NASDAQ (■); DJIA (■); DAX (■) and FTSEMIB (■). The weights refer to the volatility series estimated according to Eq. (17) respectively with window $T = 180s$ (a), $T = 360s$ (b) and $T = 720s$ (c).

sistently with the different behavior of the functionals $\mathcal{D}(\tau_j, n)$ and $\mathcal{S}(\tau_j, n)$, one can note a different dependence of the weights on the volatility window T . The volatility plays a minor role as the volatility window T increases, i.e. when the functional $\mathcal{D}(\tau_j, n)$ is less sensitive to the distance between the probability distributions P and Q . Hence the relative cluster weights $w_{i,\mathcal{D}}$ take values closer to the uniform u_i distribution with larger volatility windows T .

For the sake of clarity, a numerical example of wealth allocation is provided. Let's consider a total allocated wealth W as a net investment after taxation and commissions. The portfolio built using the Kullback-Leibler weights $w_{i,\mathcal{D}}$ is compared with those obtained by maximizing the Sharpe ratio w_i according to Markowitz theory and the uniformly distributed weights u_i . Two types

of investor strategies are considered:

- a:** *lazy investor* keeping the portfolio shares unchanged over the year. The wealth is allocated the first day of the year to the weights of the month one $\mathcal{M} = 1$. Then the portfolio weights are left unchanged. The portfolio value changes only due to the price changes of the assets.
- b:** *active investor* regularly updating the portfolio shares (monthly in our example). Specifically, the wealth is re-allocated to each index shares according to the updated portfolio weights of the corresponding period \mathcal{M} ;

In the case of the lazy investor the number of shares of each index in the portfolio does not change during the

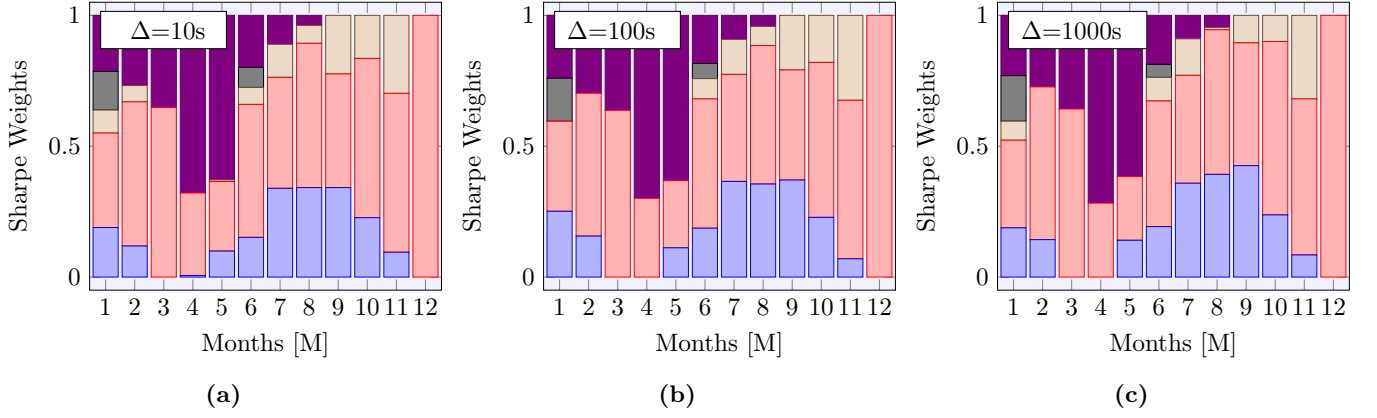


FIG. 6: **Sharpe weights w_i vs. investment horizon \mathcal{M} (monthly periods).** The weights have been estimated according to the Markowitz approach and Sharpe ratio maximization respectively for the realized volatility of the tick-by-tick data of the markets: S&P500 (■); NASDAQ (■); DJIA (■); DAX (■) and FTSEMIB (■). The three graphs correspond respectively to sampling frequency $\Delta = 10s$ (a), $\Delta = 100s$ (b), $\Delta = 1000s$ (c).

Cluster entropy weights $w_{i,\mathcal{D}}$						Sharpe Ratio weights w_i					
\mathcal{M}	S&P500	NASDAQ	DJIA	DAX	FTSEMIB	\mathcal{M}	S&P500	NASDAQ	DJIA	DAX	FTSEMIB
1	0.2229	0.2707	0.2177	0.2066	0.082	1	0.1893	0.3611	0.0877	0.1475	0.2144
2	0.2075	0.2708	0.2227	0.198	0.101	2	0.1187	0.5508	0.0622	0	0.2683
3	0.2071	0.2659	0.223	0.2044	0.0996	3	0	0.6477	0	0	0.3523
4	0.212	0.2627	0.2136	0.1871	0.1247	4	0.0061	0.3151	0	0	0.6787
5	0.2103	0.253	0.2022	0.2049	0.1296	5	0.0994	0.2657	0.0062	0	0.6288
6	0.2067	0.2577	0.2153	0.1894	0.1308	6	0.1518	0.5080	0.0648	0.0770	0.1985
7	0.2009	0.2654	0.2037	0.1945	0.1355	7	0.3392	0.4240	0.1261	0	0.1107
8	0.1996	0.2742	0.2006	0.1958	0.1298	8	0.3418	0.5513	0.0683	0	0.0386
9	0.1996	0.2737	0.1959	0.1944	0.1363	9	0.3419	0.4343	0.2238	0	0
10	0.1985	0.2697	0.2017	0.1887	0.1414	10	0.2269	0.6085	0.1645	0	0
11	0.1966	0.2759	0.1894	0.1899	0.1482	11	0.0950	0.6070	0.2980	0	0
12	0.1934	0.2758	0.1894	0.1837	0.1577	12	0	1	0	0	0

TABLE II: (Left) **Kullback-Leibler cluster entropy weights $w_{i,\mathcal{D}}$** ; The first column includes the investments horizon \mathcal{M} ranging from one to twelve months. The weights are obtained by using Eqs. (14,15) for the realized volatility series respectively for the tick-by-tick series of the markets: S&P500, NASDAQ, DJIA, FTSEMIB and DAX. The realized volatility is estimated according to Eq. (17) with window $T = 180s$. (Right) **Sharpe Ratio weights (Markowitz) w_i** . The first column includes the investments horizon \mathcal{M} ranging from one to twelve months. The weights have been estimated according to the Markowitz approach and Sharpe ratio maximization for the realized volatility of the tick-by-tick data (sampled with frequency $\Delta = 10s$)

year, whereas in the case of the active investor the number of shares of each index is updated every month evaluating the initial wealth allocated to each index (dividing W_0 by the weight of the corresponding month) dividing by the price of each index of the corresponding month.

The expected profits are estimated by considering the adjusted close prices of the five indexes on the first available day of each month of the year 2018. The adjusted prices $p_1, p_2 \dots p_{12}$ are given in US dollars and are reported in Table I. The adjusted close prices are publicly available on platforms like Yahoo finance, Google finance, Bloomberg.

By using the uniform weights $u_i = 0.2$ for all i and for all \mathcal{M} , the Kullback-Leibler weights $w_{i,\mathcal{D}}$ (Table II left) and the Sharpe ratio weights w_i (Table II right) the initial wealth $W_0 = 500000$ USD has been allocated at the first month. The number of shares of each index is

evaluated by taking the ratio of the amount of wealth allocated to each index to the price p_1 , at the beginning of the period $\mathcal{M} = 1$. The value of the portfolio is evaluated each month considering the number of shares of each index times the price at the end of the month approximated with the price at the beginning of the next month. Table III shows the portfolios' evaluated for the six cases, i.e. the two strategies (lazy and active) and three different weights (uniform, Kullback-Leibler or Sharpe ratio). The portfolio value is evaluated as the sum of the wealth allocated to each index in the portfolio. The monthly profit is evaluated as the difference between the portfolio value $W_{\mathcal{M}}$ at each month and the initially allocated wealth W_0 . Table IV shows the profit or loss in the six cases. It is worth noting that the Kullback-Leibler weights portfolio shows the best performances both with the active and lazy investor strategy compared to the equally weighted

and Markowitz portfolio.

V. CONCLUSIONS

In this work, we have shown how the relative cluster entropy can quantify the divergence between the probability distribution of the coarse grained time series of the realized volatility defined by Eq. (17) and a reference probability distribution estimated over a model time series (a simple random walk with $H = 0.5$). The volatility series is estimated for each market (S&P500, DJIA, NASDAQ, DAX, FTSEMIB) over multiple time scales τ_j and investment periods \mathcal{M} . The results are consistent with a value of the correlation exponent $H > 0.5$. There is a great interest in the financial research community in investigating volatility as a fractional Brownian motion and in particular whether the volatility can be considered a rough/smooth process see the discussion in Ref. [24, 25].

A dynamic investment strategy has been proposed by exploiting the features of the relative cluster entropy approach. Importantly, the proposed approach of portfolio construction does not rely on flawed assumptions on the market data such as normal and stationary distributions needed to apply the Markowitz and Sharpe ratio approach.

It is worth remarking that the current study differs from the analysis reported in Ref. [18] mainly addressed to demonstrate the relative cluster entropy methodology.

Then as a case study the approach has been implemented on price series that are commonly considered to behave as simple uncorrelated Brownian motions with $H \sim 0.5$.

The outcome of this work relies on the Kullback-Leibler divergence via coarse graining of sequences of power-law distributions of fractional stochastic processes with specific focus on the time series of the realized volatility. The Kullback-Leibler divergence is a pillar of the classical and quantum information theory ([1, 40]). Extensions of this research can be envisioned in different directions. Other distance measures between probability distributions have been proposed, for example the Malanobis distance, which can be used to analyse the probability distributions of sequence clustering. Another generalization of interest is the application of the proposed information measure to chaotic dynamics [41]. One estimator of chaotic system stability is the Allan variance σ_{Allan} (e.g. in fault detection, epileptic seizures from electroencephalography (EEG), stability of electronic oscillators, etc) a coarse grained multiscaled mapping of the sequences. An interesting future topic might be the application of the relative cluster entropy and minimum relative entropy principle to the probability distribution function $P(\sigma_{Allan})$.

ACKNOWLEDGMENTS

This work received financial support from the TED4LAT project (a WIDERA initiative within the Horizon Europe Programme, Grant Agreement: 101079206).

-
- [1] Vlatko Vedral. The role of relative entropy in quantum information theory. *Reviews of Modern Physics*, 74(1):197, 2002.
 - [2] D Anderson and K Burnham. Model selection and multi-model inference. *Second*. NY: Springer-Verlag, 63(2020):10, 2004.
 - [3] Édgar Roldán and Juan MR Parrondo. Entropy production and Kullback-Leibler divergence between stationary trajectories of discrete systems. *Physical Review E*, 85(3):031129, 2012.
 - [4] Akihisa Ichiki. Performance-guaranteed regularization in maximum likelihood method: Gauge symmetry in Kullback-Leibler divergence. *Physical Review E*, 108(4):044134, 2023.
 - [5] Rikab Gambhir, Benjamin Nachman, and Jesse Thaler. Learning uncertainties the frequentist way: Calibration and correlation in high energy physics. *Physical review letters*, 129(8):082001, 2022.
 - [6] Michael C Mackey. The dynamic origin of increasing entropy. *Reviews of Modern Physics*, 61(4):981, 1989.
 - [7] François Bavaud. Information theory, relative entropy and statistics. In *Formal theories of information: From Shannon to semantic information theory and general concepts of information*, pages 54–78. Springer, 2009.
 - [8] James P Crutchfield. Between order and chaos. *Nature Physics*, 8(1):17–24, 2012.
 - [9] P. Grassberger and I. Procaccia. Characterization of strange attractors. *Phys. Rev. Lett.*, 50(5):346, 1983.
 - [10] Erhan Gokcay and Jose C. Principe. Information theoretic clustering. *IEEE transactions on pattern analysis and machine intelligence*, 24(2):158–171, 2002.
 - [11] Anil K Jain. Data clustering: 50 years beyond k-means. *Pattern recognition letters*, 31(8):651–666, 2010.
 - [12] Nguyen Xuan Vinh, Julien Epps, and James Bailey. Information theoretic measures for clusterings comparison: Variants, properties, normalization and correction for chance. *Journal of Machine Learning Research*, 11:2837–2854, 2010.
 - [13] Alex Rodriguez and Alessandro Laio. Clustering by fast search and find of density peaks. *science*, 344(6191):1492–1496, 2014.
 - [14] James Bailey, Michael E. Houle, and Xingjun Ma. Relationships between tail entropies and local intrinsic dimensionality and their use for estimation and feature representation. *Information Systems*, 118:102245, 2023.
 - [15] A. Carbone, G. Castelli, and H. E. Stanley. Analysis of clusters formed by the moving average of a long-range correlated time series. *Physical Review E*, 69:026105, Feb 2004.
 - [16] A. Carbone and H. E. Stanley. Scaling properties and entropy of long-range correlated time series. *Physica A: Statistical Mechanics and its Applications*, 384(1):21–24,

Uniform portfolio (Not updated)							Uniform portfolio (Monthly updated)						
\mathcal{M}	SPX	NASDAQ	DJIA	DAX	FTSE	Portfolio	\mathcal{M}	SPX	NASDAQ	DJIA	DAX	FTSE	Portfolio
1	104680	105408	105489	104801	97550	517929	1	104680	105408	105489	104801	97550	517929
2	99327	102478	99133	95198	97933	494071	2	94886	97220	93975	90836	100393	477311
3	95773	98047	95247	94626	97979	481675	3	96422	95676	96079	99399	100046	487625
4	98478	101766	97079	96722	100684	494731	4	102824	103792	101923	102215	102760	513516
5	101439	107812	99239	95350	88156	491998	5	103006	105940	102224	98581	87557	497311
6	101146	108003	97918	91844	90873	489786	6	99710	100176	98668	96322	103082	497961
7	104360	109995	102053	95198	87263	498872	7	103177	101844	104223	103651	96027	508925
8	107452	115475	104545	90929	8401	502421	8	102963	104981	102442	95516	96279	502183
9	108486	114705	107360	91653	79058	501265	9	100962	99333	102692	100796	94097	497881
10	101652	106096	102242	83803	77615	471410	10	93700	92494	95232	91434	98174	471037
11	103507	106202	104038	83498	75913	473160	11	101824	100100	101756	99636	97807	501124
12	93108	95133	94047	77134	77771	437195	12	89953	89577	90396	92377	102447	464753

Kullback-Leibler portfolio (Not updated)							Kullback-Leibler portfolio (Monthly updated)						
\mathcal{M}	SPX	NASDAQ	DJIA	DAX	FTSE	Portfolio	\mathcal{M}	SPX	NASDAQ	DJIA	DAX	FTSE	Portfolio
1	116666	142670	114825	108260	39995	522417	1	116666	142670	114825	108260	39995	522417
2	110700	138704	107907	98339	40152	495804	2	98444	131636	104641	89928	50698	475348
3	106739	132707	103676	97749	40171	481045	3	99845	127202	107128	101586	49823	485586
4	109754	137741	105671	99914	41280	494362	4	108993	136332	108854	95622	64071	513873
5	113054	145924	108022	98497	36144	501642	5	108311	134015	103349	100996	56737	503409
6	112727	146182	106583	94875	37258	497627	6	103051	129077	106216	91217	67415	496979
7	116309	148879	111085	98339	35778	510392	7	103642	135147	106151	100801	65058	510801
8	119756	156296	113798	93930	34447	518228	8	102757	143930	102749	93510	62485	505432
9	120908	155253	116862	94678	32414	520116	9	100760	135937	100587	97974	64127	499386
10	113292	143601	111291	86568	31822	486576	10	92998	124728	96042	86268	69409	469447
11	115359	143745	113245	86253	31124	489728	11	100093	138088	96362	94604	72475	501624
12	103769	128763	102370	79679	31886	446469	12	86984	123527	85605	84849	80779	461747

Sharpe ratio portfolio (Not updated)							Sharpe ratio portfolio (Monthly updated)						
\mathcal{M}	SPX	NASDAQ	DJIA	DAX	FTSE	Portfolio	\mathcal{M}	SPX	NASDAQ	DJIA	DAX	FTSE	Portfolio
1	99057	190305	46281	77311	104561	517517	1	99057	190305	46281	77311	104561	517517
2	93992	185016	43493	70226	104972	497700	2	56336	267728	29242	0	134653	487961
3	90629	177017	41788	69805	105021	484261	3	0	309845	0	0	176236	486081
4	93189	183731	42592	71351	107920	498784	4	3153	163536	0	0	348741	515431
5	95991	194646	43539	70339	94492	499009	5	51189	140727	3157	0	275263	470337
6	95713	194990	42960	67752	97405	498822	6	75656	254453	31943	37075	102314	501442
7	98755	198587	44774	70226	93535	505880	7	174985	215907	65719	0	53152	509764
8	101681	208481	45867	67078	90055	513164	8	175966	289390	34977	0	18577	518912
9	102659	207091	47102	67612	84740	509206	9	172592	215725	114889	0	0	503208
10	96193	191547	44857	61820	83193	477613	10	106321	281430	78342	0	0	466094
11	97948	191739	45645	61595	81369	478299	11	48378	303812	151596	0	0	503787
12	88107	171756	41261	56901	83361	441388	12	0	447888	0	0	0	447888

TABLE III: Wealth montly allocated to the five indexes. The total wealth allocated is reported in the last column.

- 2007.
- [17] A. Carbone. Information measure for long-range correlated sequences: the case of the 24 human chromosomes. *Scientific Reports*, 3:2721, 2013.
- [18] Anna Carbone and Linda Ponta. Relative cluster entropy for power-law correlated sequences. *SciPost Physics*, 13(3):076, 2022.
- [19] David Backus, Mikhail Chernov, and Stanley Zin. Sources of entropy in representative agent models. *The Journal of Finance*, 69(1):51–99, 2014.
- [20] Anisha Ghosh, Christian Julliard, and Alex P. Taylor. What Is the Consumption-CAPM Missing? An Information-Theoretic Framework for the Analysis of Asset Pricing Models. *Review of Financial Studies*, 30(2):442–504, FEB 2017.
- [21] M. Ormos and D. Zibriczky. Entropy-based financial asset pricing. *PLoS ONE*, 9(12):e115742, 2014.
- [22] Anil K Bera and Sung Y Park. Optimal portfolio diversification using the maximum entropy principle. *Econometric Reviews*, 27(4-6):484–512, 2008.
- [23] Michele Tumminello, Fabrizio Lillo, and Rosario N Mantegna. Kullback-Leibler distance as a measure of the information filtered from multivariate data. *Physical Review E*, 76(3):031123, 2007.
- [24] Fabienne Comte and Eric Renault. Long memory in continuous-time stochastic volatility models. *Mathematical finance*, 8(4):291–323, 1998.
- [25] Jim Gatheral, Thibault Jaisson, and Mathieu Rosenbaum. Volatility is rough. *Quantitative Finance*, 18(6):933–949, 2018.
- [26] Rama Cont and Purba Das. Rough volatility: fact or artefact? *Sankhya B*, pages 1–33, 2024.
- [27] Mark O Hill. Diversity and evenness: a unifying notation and its consequences. *Ecology*, 54(2):427–432, 1973.

\mathcal{M}	Profit					
	Uniform		Kullback-Leibler		Sharpe ratio	
	(a)	(b)	(a)	(b)	(a)	(b)
1	17929	17929	22417	22417	17517	17517
2	-5928	-22688	-4195	-24651	-2299	-12038
3	-18324	-12374	-18954	-14413	-15738	-13918
4	-5268	13516	-5637	13873	-1215	15431
5	-8001	-2688	1642	3409	-990	-29662
6	-10213	-2038	-2372	-3020	-1177	1442
7	-1127	8925	10392	10801	5880	9764
8	2421	2183	18228	5432	13164	18912
9	1265	-2118	20116	-613	9206	3208
10	-28589	-28962	-13423	-30552	-22386	-33905
11	-26839	1124	-10271	1624	-21700	3787
12	-62804	-35246	-53530	-38252	-58611	-52111
Year	-145480	-62438	-35589	-53944	-78351	-71571

TABLE IV: Profit or loss of the six portfolios considered. The values are evaluated as the difference between the portfolios' values and the initial quantity of wealth invested.

- [28] Tom Leinster and Emily Roff. The maximum entropy of a metric space. *The Quarterly Journal of Mathematics*, 72(4):1271–1309, 2021.
- [29] Vihang Errunza, Basma Majerbi, and Maxwell Tuuli. Learning from biodiversity: Is diversity in financial ecosystems important for economic growth and stability? *IMF Economic Review*, pages 1–60, 2024.
- [30] Harry Markowitz. Portfolio selection. *The Journal of Finance*, 7(1):77–91, 1952.
- [31] Nils H Hakansson. Multi-period mean-variance analysis: Toward a general theory of portfolio choice. *The Journal of Finance*, 26(4):857–884, 1971.
- [32] Marc C Steinbach. Markowitz revisited: Mean-variance models in financial portfolio analysis. *SIAM review*, 43(1):31–85, 2001.
- [33] Sidney Redner. *A guide to first-passage processes*. Cambridge university press, 2001.
- [34] Mingzhou Ding and Weiming Yang. Distribution of the first return time in fractional brownian motion and its application to the study of on-off intermittency. *Physical Review E*, 52(1):207, 1995.
- [35] Ole E Barndorff-Nielsen and Neil Shephard. Econometric analysis of realized volatility and its use in estimating stochastic volatility models. *Journal of the Royal Statistical Society Series B: Statistical Methodology*, 64(2):253–280, 2002.
- [36] Torben G Andersen, Tim Bollerslev, Francis X Diebold, and Paul Labys. Modeling and forecasting realized volatility. *Econometrica*, 71(2):579–625, 2003.
- [37] Linda Ponta and Anna Carbone. Information measure for financial time series: Quantifying short-term market heterogeneity. *Physica A: Statistical Mechanics and its Applications*, 510:132 – 144, 2018.
- [38] Pietro Murialdo, Linda Ponta, and Anna Carbone. Inferring multi-period optimal portfolios via detrending moving average cluster entropy. *Europhysics letters*, 133(6):60004, 2021.
- [39] Paolo Brandimarte. *Numerical methods in finance and economics: a MATLAB-based introduction*. John Wiley & Sons, 2013.
- [40] A Kowalewska-Kudłasyk, JK Kalaga, W Leoński, and V Cao Long. Kullback–Leibler quantum divergence as an indicator of quantum chaos. *Physics Letters A*, 376(15):1280–1286, 2012.
- [41] Naoki Asuke, Nicolas Chauvet, André Röhm, Kazutaka Kanno, Atsushi Uchida, Tomoaki Niiyama, Satoshi Sunada, Ryoichi Horisaki, and Makoto Naruse. Analysis of temporal structure of laser chaos by Allan variance. *Physical Review E*, 107(1):014211, 2023.